



**HAL**  
open science

## AI-supported Modelling of a Simple TPR System for Fusion Neutron Measurement

V. Gerenton, A. Jardin, U. Wiącek, K. Drozdowicz, A. Kulinska, A. Kurowski, M. Scholz, U. Woźnicka, W. Dąbrowski, B. Łach, et al.

► **To cite this version:**

V. Gerenton, A. Jardin, U. Wiącek, K. Drozdowicz, A. Kulinska, et al.. AI-supported Modelling of a Simple TPR System for Fusion Neutron Measurement. *Journal of Fusion Energy*, 2024, 43 (1), pp.10. 10.1007/s10894-024-00403-0 . hal-04874081

**HAL Id: hal-04874081**

**<https://hal.science/hal-04874081v1>**

Submitted on 8 Jan 2025

**HAL** is a multi-disciplinary open access archive for the deposit and dissemination of scientific research documents, whether they are published or not. The documents may come from teaching and research institutions in France or abroad, or from public or private research centers.

L'archive ouverte pluridisciplinaire **HAL**, est destinée au dépôt et à la diffusion de documents scientifiques de niveau recherche, publiés ou non, émanant des établissements d'enseignement et de recherche français ou étrangers, des laboratoires publics ou privés.



Distributed under a Creative Commons Attribution 4.0 International License



# AI-supported Modelling of a Simple TPR System for Fusion Neutron Measurement

V. Gerenton<sup>1</sup> · A. Jardin<sup>2</sup> · U. Wiącek<sup>2</sup> · K. Drozdowicz<sup>2</sup> · A. Kulinska<sup>2</sup> · A. Kurowski<sup>2</sup> · M. Scholz<sup>2</sup> · U. Woźnicka<sup>2</sup> · W. Dąbrowski<sup>3</sup> · B. Łach<sup>3</sup> · D. Mazon<sup>4</sup>

Accepted: 3 April 2024 / Published online: 23 April 2024  
© The Author(s) 2024

## Abstract

The system proposed to measure the tritium to deuterium ratio on the International Thermonuclear Experimental Reactor (ITER) is a high-resolution neutron spectrometer, partly composed of a system of three Thin-foil Proton Recoil (TPR) spectrometers. This system works on the principle of converting neutrons into protons using a thin foil of polyethylene, which is then detected in silicon detectors to obtain the scattering angles and energy spectrum of the protons. The objective of this article is to show the benefit of artificial intelligence for improving a simple TPR system model written in Python to an accuracy approaching MCNP simulations, while significantly decreasing the computational cost. The first step was to model a polyethylene converter to obtain the energy-angle distribution of outgoing protons for a given incident neutron beam. When compared with MCNP, this simplified model was found to fail to account for proton energy and angular scattering. Therefore, in a second step, two neural networks were successfully trained to include these effects based on the output data of the TRIM code, assuming Gaussian distributions. The Python model was able to produce results very close (differences up to a few percent) to those obtained with MCNP by integrating these neural networks. To extend the study, the energy spectra of the protons could be obtained and subsequently used to obtain information on the ratio of deuterium and tritium in the plasma.

**Keywords** Fusion plasmas · Neutron spectrometry · Thin-foil proton recoil · Ion matter interaction · Diagnostic design

## Introduction

Diagnostic systems play a crucial role in machine protection, plasma control, performance, and physical studies. One essential parameter is the fuel ratio, denoted as the relative quantity of tritium and deuterium  $n_t/n_d$  in the plasma, which is measured using neutron spectroscopy. Various neutron diagnostics will be available on ITER, including

the Radial Neutron Camera (RNC), Vertical Neutron Camera (VNC), MicroFission Chambers (MFC), Neutron Flux Monitor (NFM), Divertor Neutron Flux Monitors (DNFM), Neutron Activation System (NAS) and High-Resolution Neutron Spectrometer (HRNS) [1]. In this paper, our main interest lies in HRNS since this diagnostic is well-suited for the measurement of the core plasma fuel ratio.

The HRNS system of ITER is designed to operate in a range of plasma scenarios, from pure D-discharge to full-power DT-discharge [2]. The TPR spectrometer is the part of the HRNS system designed specifically for ITER high-power DT plasma discharges. The operating principle of the TPR spectrometer involves a collimated neutron beam interacting with a thin foil of hydrogen-rich polyethylene (PE) and two annular silicon (Si) detectors in a dE-E configuration [3]. The collimated neutron beam undergoes elastic scattering on the hydrogen nuclei in the foil, producing recoil protons with energy  $E_p$  determined by the energy of the incoming neutron  $E_n$  and the scattering angle of the proton  $\theta$ , such that:  $E_p = E_n \cos^2 \theta$ .

✉ A. Jardin  
axel.jardin@ifj.edu.pl

V. Gerenton  
valentin.gerenton42@gmail.com

<sup>1</sup> ENSICAEN, Caen 14000, France

<sup>2</sup> Institute of Nuclear Physics, Polish Academy of Sciences (IFJ PAN), Radzikowskiego 152, Krakow PL-31-342, Poland

<sup>3</sup> Faculty of Physics and Applied Computer Science, AGH University of Krakow, Krakow, Poland

<sup>4</sup> CEA, IRFM, Saint-Paul-lez-Durance F-13108, France

Subsequently, some of the recoil protons deposit their energy in annular Si detectors placed after the foil. Simulations tools like GEANT4 [4], MCNP [5], and PROTON [6], have been employed to assess the spectrometer performance, such as energy resolution, detection efficiency or count rate capabilities [2]. However, these simulation tools are computationally expensive, and difficult to use for design. In this article, a simple TPR model written in Python will be studied. The purpose is to develop a fast but efficient model that allows to quickly estimate proton absorption and scattering in material for different energies and thickness, supporting the optimization of the diagnostic design and the evaluation of detector performance. The rest of the paper is as follows. In section two, the model and method used to calculate the neutron-proton (n-p) conversion efficiency and the proton energy-angle distribution in the PE foil are described. In the third section, the implementation of proton angular and energy scattering with Gaussian fits of TRIM [7] simulation outputs is explained. In the fourth section, two neural networks are designed and trained to reproduce proton scattering for any incident energy and material thickness. In section five, a comparison with MCNP results is made. Finally, conclusions and perspectives are presented in the last section.

## Thin-Foil Polyethylene (PE) Neutron-Proton Converter

The distribution of ejected protons was obtained by considering a monoenergetic and unidirectional beam of incident neutrons reaching the PE foil, as depicted in Fig. 1.

Firstly, the n-p elastic collisions are parametrized with the assumption of hard spheres of similar radius  $R$ , for which the scattering angle  $\theta$  is given by  $\sin\theta = b/2R$ , where  $b$  is the impact parameter. Secondly, the average energy loss of protons for any initial energy and thicknesses of PE crossed was estimated by reconstructing their Bragg curve, thanks to the values of stopping power [ $\text{MeV}\cdot\text{cm}^2/\text{g}$ ] of protons in PE obtained from the NIST database [8]. For the specific needs

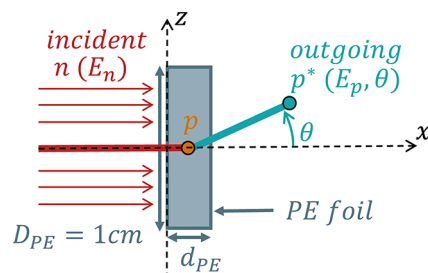


**Fig. 1** Parametrization of neutron-proton conversion in PE, with  $E_n$  the incident neutron energy,  $(E_p, \theta)$  the energy and scattering angle of outgoing protons,  $d_{PE}$  the converter thickness and  $D_{PE}$  its diameter

of this work, focused on 14 MeV D-T neutrons, the proton absorption matrix in PE is calculated for PE crossed thicknesses in the range 1  $\mu\text{m}$  to 3 mm and initial proton energies between 10 keV and 20 MeV. Moreover, the n-p conversion rate  $p$  is calculated using the formula  $p = \sigma \cdot N \cdot d_{PE}$ , where the n-p elastic collision cross-section is taken from the JENDL/HE-2007 dataset of the JANIS database [9], and  $N$  is the density of protons in PE ( $N \approx 7.98 \cdot 10^{28} \text{ m}^{-3}$  for a density of  $0.93 \text{ g/cm}^3$ ), and  $d_{PE}$  is the PE thickness. Finally, by defining probability distributions of the n-p collision parameters in the PE, i.e. the collision position  $0 < x < d_{PE}$  and the impact parameter  $0 < b/R < 2$ , it is therefore possible to calculate numerically, with a Monte-Carlo approach, the 2D matrix of the proton energy-angle distribution at the outlet of a PE foil with a given thickness, as presented in Fig. 2 for  $d_{PE} = 0.1 \text{ mm}$  and  $1.0 \text{ mm}$ .

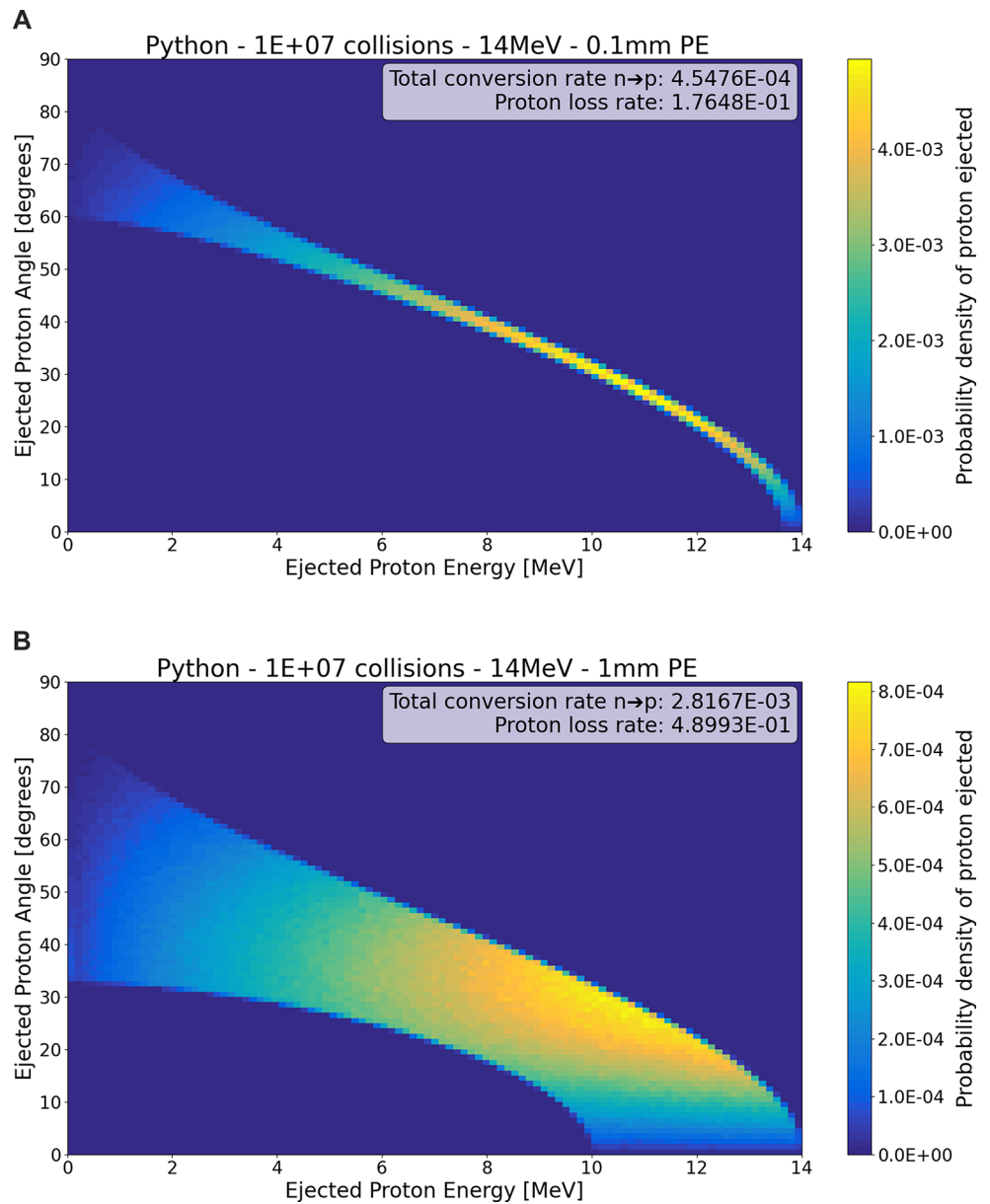
Additionally, the total n-p conversion rate of the PE foil, including proton absorption, can be calculated using the formula  $p_{tot} = \frac{N_{pout}}{N_n}$ , where  $N_{pout}$  is the total number of protons leaving the PE and  $N_n$  is the number of incident neutrons. One objective here is to study the influence of PE thickness on the total n-p conversion rate, which can be obtained by running simulations for various thicknesses, as shown in Fig. 3.

Figure 3 shows a remarkable agreement with MCNP results, demonstrating the robustness of this approach. Some discrepancy arises at thicknesses larger than 1 mm, as part of the incident neutron beam is scattered in the PE, a phenomenon which is neglected (thin-foil assumption) in the Python model. To determine the optimum PE thickness, a compromise must be found between maximizing the conversion rate and minimizing proton energy absorption in the PE. From Figs. 2 and 3, it can be deduced that the range of interest lies between 0.1 and 1.0 mm. In the following sections, we concentrate on a 1.0 mm PE converter because scattering effects are more visible at higher thicknesses.

## Gaussian Fitting of TRIM Output Distributions

In the previous step, only the average values of individual proton trajectories in terms of energy and angle were considered, without accounting for statistical fluctuations. To estimate this scattering effect, the freely available online SRIM/TRIM code was utilized [7]. The TRIM software allows specifying the energy of the incident particles and the number of particles (protons in this case), along with the composition and thickness of the layer traversed. An output file containing the energy and angle values of each proton can be obtained, and was used to generate histograms for the energy and angle distributions of the transmitted protons, as

**Fig. 2** Proton energy-angle distribution exiting a PE foil with a thickness of 0.1 mm (a) and 1.0 mm (b)



**Fig. 3** Total n-p conversion rate as a function of PE thickness, as calculated by MCNP and with the Python model

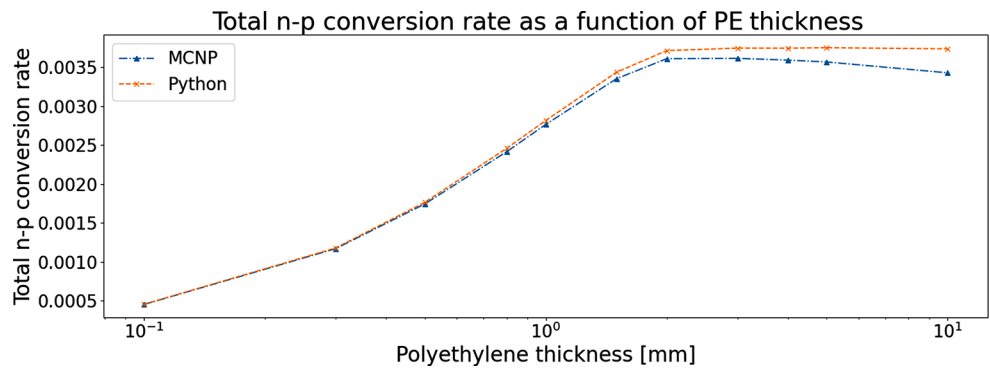


**Fig. 4** Histogram of the proton energy distribution approximated by a Gaussian function

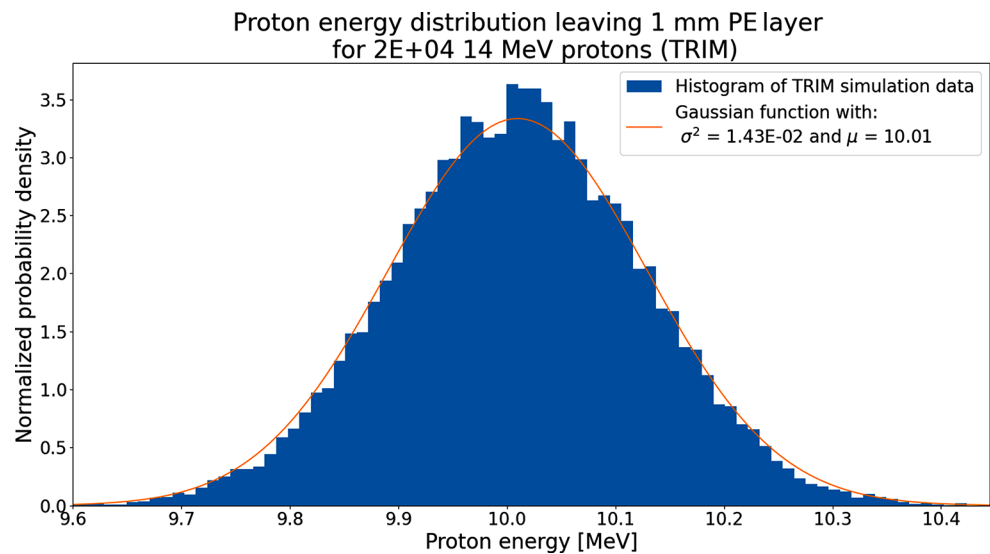
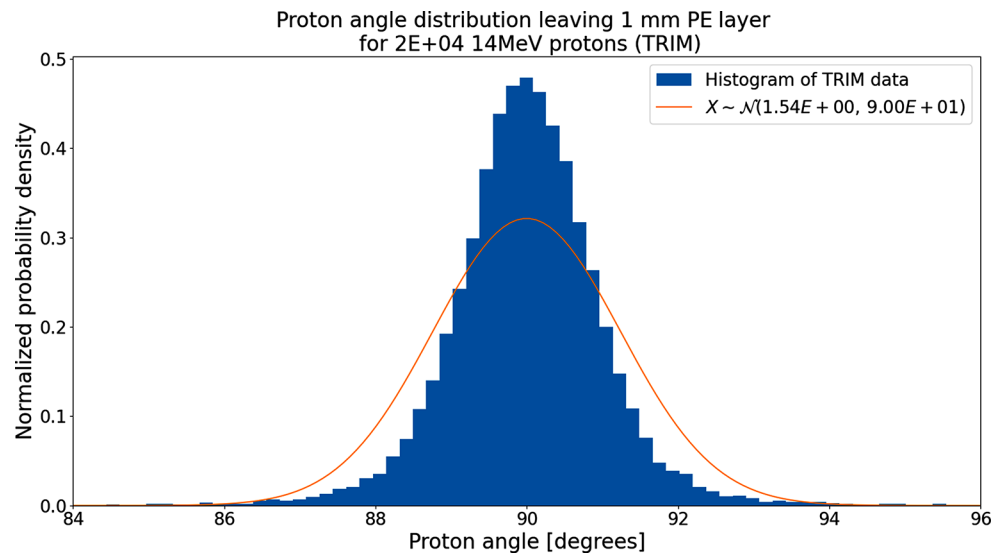


**Fig. 5** Histogram of the proton angular distribution approximated by a Gaussian function



shown in Figs. 4 and 5. Due to the Gaussian-like shape of the histograms, the mean  $\mu$  and variance  $\sigma^2$  of these data sets were extracted to fit the distributions with Gaussian functions [10]. The histogram of the angle distribution shows that the energy scattering does not exactly correspond to a Gaussian function. However, to avoid applying corrections that would likely vary for each thickness and each energy value, the  $\mu$  and  $\sigma$  values are used to simplify the calculations, which provided satisfying results.

To obtain the energy and the angular scattering distribution, 60 simulations were conducted with thickness ranging from 0.001 mm to 2 mm and energy ranging from 9 keV to 66.5 MeV, as depicted in Figs. 6 and 7. To quantify the impact of energy and angular scatterings on the proton distributions, the decision was made to use specific figures of merit. For energy scattering, the Full Width at Half Maximum (FWHM) normalized by the mean energy ( $E_{mean}$ ) was

calculated, while the standard deviation ( $\sigma$ ) was directly used for angular scattering.

However, obtaining these values for all thicknesses and energies within our domain of interest could not be achieved using simple polynomial or exponential fitting functions and including TRIM directly in the python code would be too computationally expensive, indicating that artificial intelligence tools might be adapted to this problem.

## Integration of Neural Networks (NN)

Therefore, Neural Networks (NN), as presented in Fig. 8, were utilized in order to reproduce and interpolate proton scattering effects calculated by TRIM. It is worth noting that this solution has already been successfully applied to a similar problem presented in [11]. The function sklearn.

**Fig. 6** Proton scattering in energy  $\frac{FWHM}{E_{mean}}$  obtained with TRIM for several values of proton energies and PE thicknesses

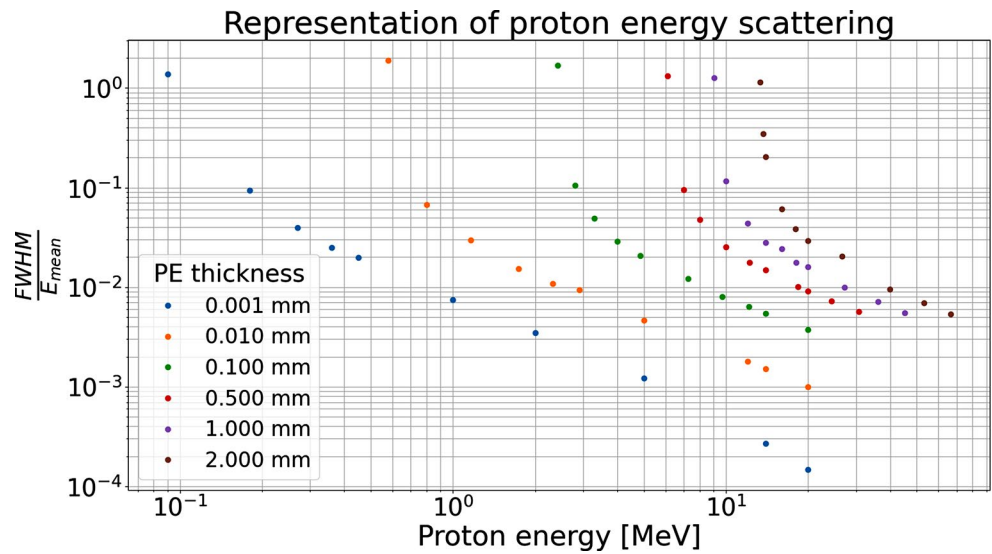


**Fig. 7** Proton angular scattering ( $\sigma$ ) for each considered TRIM data point

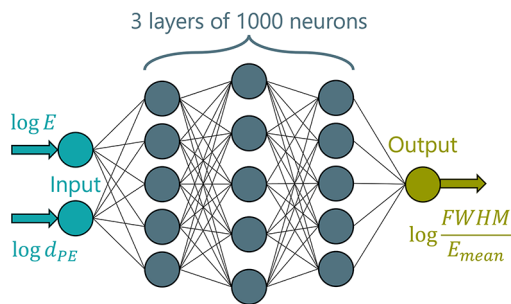
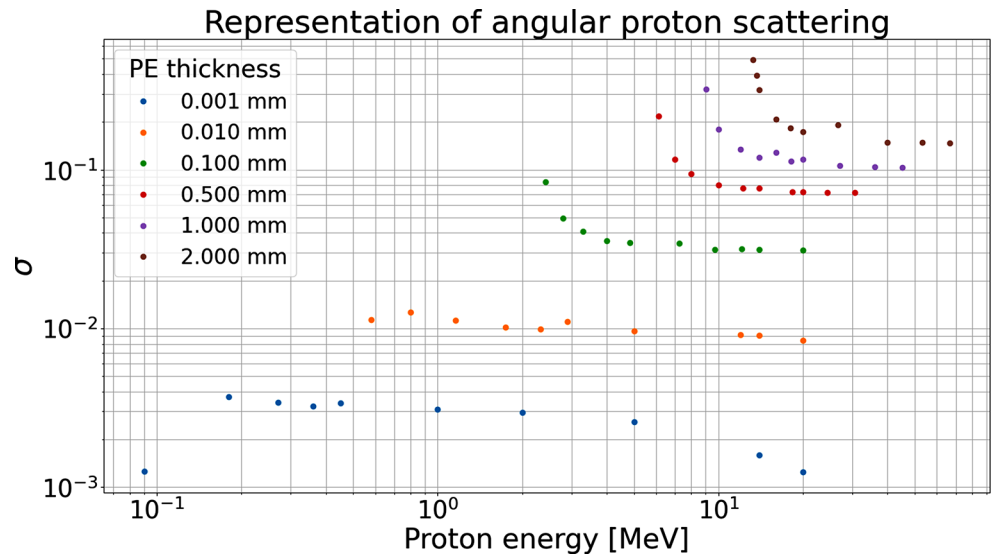


**Fig. 8** Model of the NN used. The inputs are the logarithms of the initial proton energy ( $E$ ) and of the PE thickness ( $d_{PE}$ ), and outputs are the logarithms of the figures of merit for the energy or angular scattering

neural\_network.MLPRegressor from the sci-kit-learn library [12] was employed for optimization, using the Limited-memory Broyden–Fletcher–Goldfarb–Shanno (LBFGS) solver, as described in [13]. For small datasets,

'LBFGS' is preferred due to faster convergence and better performance. The Rectified Linear Unit (ReLU) activation function, as explained in [14], was chosen as it provided the best results. To ensure convergence, a large number of iterations were utilized, without leading to an overfitting of the training database. Two similar NNs of 3 fully connected hidden layers composed of 1000 neurons each were used for energy scattering and angular scattering.

The NNs are trained with data obtained from TRIM as described in the previous section, and their performance could be verified using the score function, which returns the coefficient of determination  $R^2$  defined as  $1 - \frac{u}{v}$ , where  $u$  is the residual sum of squares  $\sum ((y_{true} - y_{pred})^2)$  and  $v$  is the total sum of squares  $\sum ((y_{true} - \bar{y}_{true})^2)$  where  $y_{true}$  is the true value obtained by TRIM and  $y_{pred}$  is the value predicted by the NN model [15]. A high score closes to 1 indicates that the NN predictions are matching well the actual



values. To ensure model coherence, a dataset of 36 simulations for thicknesses of 0.003 mm, 0.02 mm and 0.1 mm and energies between 0.5 MeV and 20 MeV, not included in the training set is used for the validation step. For various thicknesses and the two NN models, as shown in Figs. 9 and 10, the NN models have respective scores of 0.992 and 0.942, indicating that both models are well-trained. As a result, they could be used to improve Python simulations with proton scattering effects.

### Comparison with MCNP Calculations

The NN training performed previously allowed the proton energy and angular scattering to be implemented in the Python code, using Gaussian random variables. Furthermore, a comparison of the results with and without NN with MCNP is shown in Fig. 11. Generally, a good agreement is found between the Python model and MCNP, with errors not exceeding a few percent (up to 7%) for most of the distribution. Only the lower edge of the energy-angle distribution exhibits local differences of up to 20% (in yellow and blue). Furthermore, the improvement when including scattering effects is evident in Fig. 11 (b), with significantly reduced differences compared to Fig. 11 (a), especially in the lower edge of the proton energy-angle distribution.

In order to better understand the impact of the different scattering mechanisms, a 4 MeV slice of the 2D proton energy-angle distribution is presented in Fig. 12 for MCNP and the Python model with and without scattering effects.

The distributions, although very similar, exhibit greater differences at low angles in the range [20°-35°]. In addition, the impact of energy diffusion alone seems negligible, demonstrating that the dominant source of discrepancy is proton angular scattering.

### Summary and Future

In this work, a PE n-p converter model was developed and written in Python language using various databases to calculate the angle-energy distribution of the recoil protons exiting the PE. Despite a general good agreement in terms of total conversion rate and global shape of the energy-angle distribution, a comparison with MCNP revealed that certain effects were not considered in this simplified model, leading to discrepancies locally exceeding 20%. Nevertheless, the code was enhanced using the TRIM software and two neural networks were trained with TRIM outputs to predict energy and angular scattering. As a result, the proton distribution was found to be weakly influenced by energy scattering and mostly influenced by angular scattering. In addition, thanks to the incorporation of these phenomena, the Python model could give results very close to MCNP, despite small remaining differences of up to 7%. In conclusion, the study has shown that the Python code, thanks to various improvements, is able to offer results close to those of powerful calculation codes such as MCNP, at a much lower computational cost.

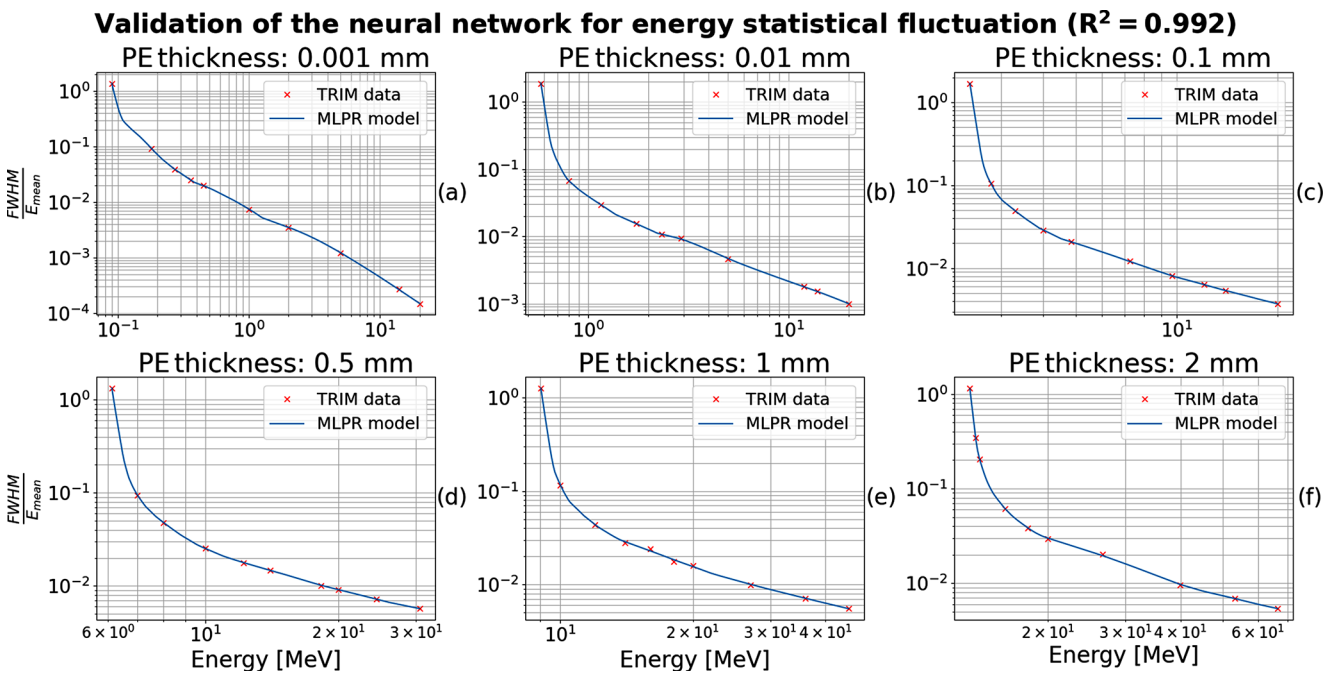
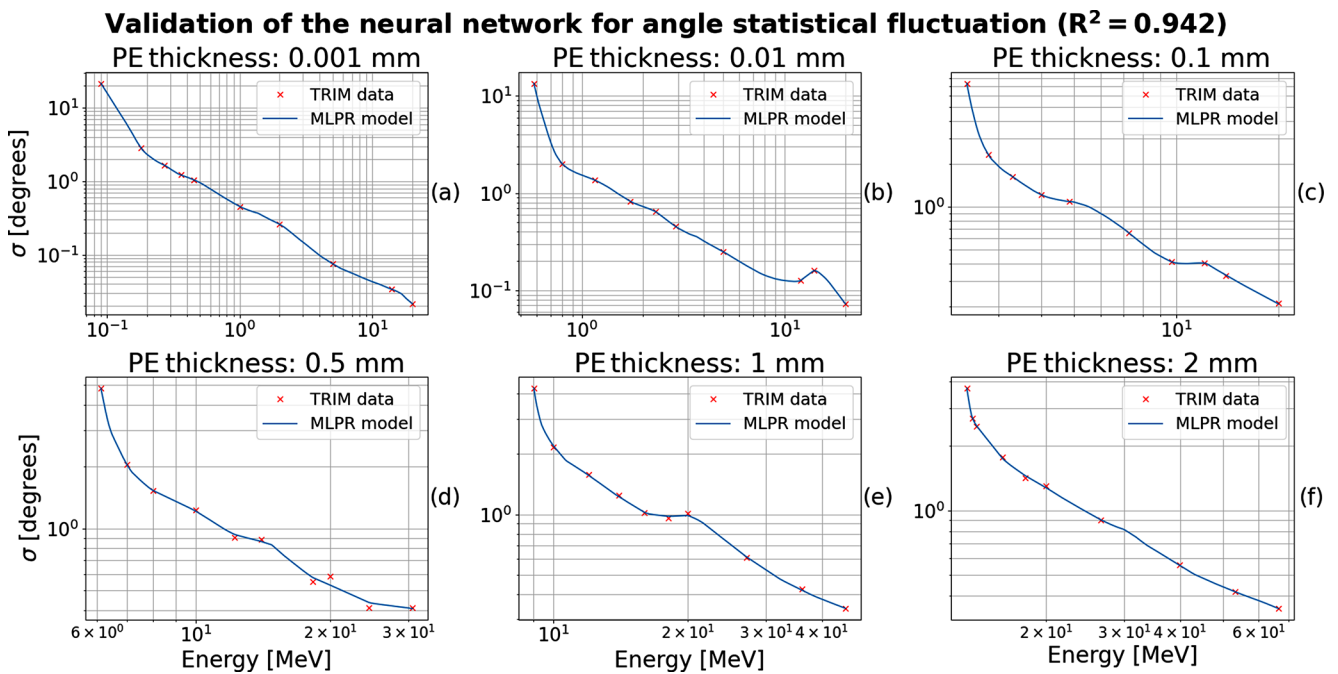


Fig. 9 Proton energy scattering  $\frac{FWHM}{E_{mean}}$  for different PE thicknesses and initial proton energies, including TRIM data and NN predictions



**Fig. 10** Angular proton scattering  $\sigma$  for different PE thicknesses and initial proton energies, including TRIM data and NN predictions

To extend the study, the energy spectra of the protons could be obtained and exploited further. Indeed, the proton energy spectrum can be used to deduce information about the incident neutrons and determine the ratio of deuterium and tritium in the plasma core of a tokamak. In addition, the TPR system could be improved by replacing the Si detectors with Gas Electron Multiplier (GEM)-type gas detectors in order to increase the lifetime of the system before maintenance is required. As mentioned previously, the system studied will be subjected to strong neutron flux, which deteriorates the silicon properties over time. A GEM-type gas detector as presented by Scholz et al. in [16] could solve this problem because of the lower vulnerability of a flowing gas to damage caused by high neutron flux.



**Fig. 11** Comparison of the Python model with MCNP for the 2D proton energy-angle distribution, after 1 mm of PE, (a) without and (b) with TRIM + NN scattering effects

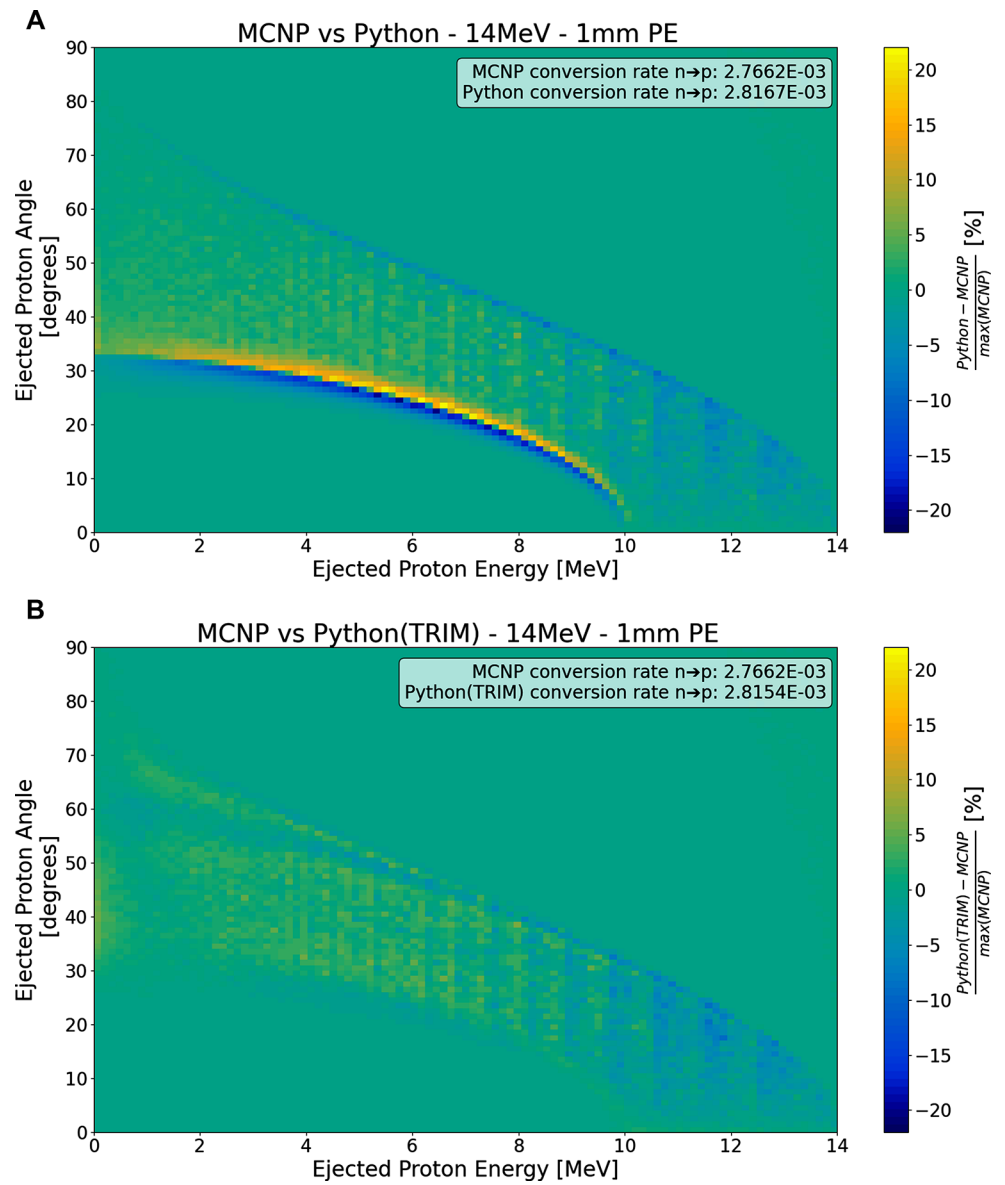
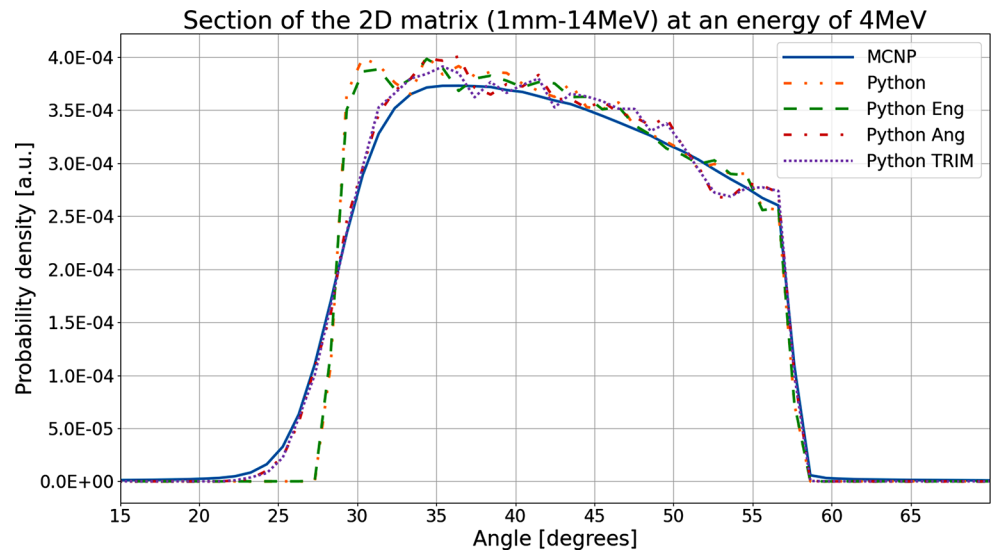


**Fig. 12** 4 MeV section of the 2D proton energy-angle distribution after 1 mm PE for MCNP and the Python code



**Acknowledgements** This work has been carried out within the framework of the EUROfusion Consortium, funded by the European Union via the Euratom Research and Training Programme (Grant Agreement No 101052200 — EUROfusion). Views and opinions expressed are however those of the author(s) only and do not necessarily reflect those of the European Union or the European Commission. Neither the European Union nor the European Commission can be held responsible for them. This project is co-financed by the Polish Ministry of Education and Science in the framework of the International Co-financed Projects (PMW) programme Contract No 5450/HEU - EURATOM/2023/2 and Contract No 5463/HEU-EURATOM/2023/2.

**Author Contributions** VG: Methodology, Formal analysis, Investigation, Writing—Original Draft, Editing. AJ: Conceptualization, Methodology, Investigation, Writing—Review, Supervision. UW: Formal analysis, Investigation, Validation, Software. KD: Conceptualization, Writing—Review, Supervision. AKul: Methodology, Investigation, Writing—Review. AKur: Resources, Formal analysis, Writing—Review. MS: Conceptualization, Writing—Review, Project administration, Funding acquisition. UW: Project administration, Funding acquisition. WD: Conceptualization, Writing—Review, Supervision, Funding acquisition. BL: Methodology, Formal analysis, Validation. DM: Conceptualization, Supervision, Writing—Review.

**Data Availability** No datasets were generated or analysed during the current study.

## Declarations

**Competing Interests** The authors declare no competing interests.

**Open Access** This article is licensed under a Creative Commons Attribution 4.0 International License, which permits use, sharing, adaptation, distribution and reproduction in any medium or format, as long as you give appropriate credit to the original author(s) and the source, provide a link to the Creative Commons licence, and indicate if changes were made. The images or other third party material in this article are included in the article's Creative Commons licence, unless indicated otherwise in a credit line to the material. If material is not included in the article's Creative Commons licence and your intended use is not permitted by statutory regulation or exceeds the permitted use, you will need to obtain permission directly from the copyright holder. To view a copy of this licence, visit <http://creativecommons.org/licenses/by/4.0/>.

## References

1. L. Bertalot et al., Fusion neutron diagnostics on ITER tokamak. *J. Instr.* **7**, C04012 (2012)
2. M. Scholz et al., Conceptual design of the high resolution neutron spectrometer for ITER. *Nucl. Fusion.* **59**, 065001 (2019)
3. B. Marcinkevicius et al., Thin foil proton recoil spectrometer performance study for application in DT plasma measurements. *Rev. Sci. Instr.* **89**, 101107 (2018)
4. J. Allison et al., Recent developments in geant4. *Nucl. Instrum. Methods Phys. Res. Sect. A: Accelerators Spectrometers Detectors Assoc. Equip.* **835**, 186–225 (2016)
5. D.B. Pelowitz (ed.), MCNPX Users Manual Version 2.7.0 LA-CP-11-00438 (2011)
6. B. Marcinkevicius et al., A thin-foil Proton Recoil spectrometer for DT neutrons using annular silicon detectors. *J. Instr.* **14**, P03007 (2019)
7. J.F. Ziegler, M.D. Ziegler, J.P. Biersack, SRIM – The stopping and range of ions in matter, Nuclear Instruments and Methods in Physics Research Section B: Beam Interactions with Materials and Atoms, vol. 268, no 11, 2010, pp. 1818–1823
8. M.J. Berger et al., Stopping-Power & Range Tables for Electrons, Protons, and Helium Ions, <https://doi.org/10.18434/T4NC7P>
9. Y. Watanabe et al., Status of JENDL High Energy file. *J. Korean Phys. Soc.* **59**(2), 1040–1045 (2011)
10. S. Tavernier, *Experimental Techniques in Nuclear and Particle Physics* (Springer, Introduction, 2010), pp. 1–22
11. Florian, Krüger et al., Machine learning plasma-surface interface for coupling sputtering and gas-phase transport simulations. *Plasma Sources Sci. Technol.* **28**, 035002 (2019)
12. F. Pedregosa et al., Scikit-learn: machine learning in Python. *J. Mach. Learn. Res.* **12**, 2825–2830 (2011)
13. D.C. Liu, J. Nocedal, On the limited memory bfgs method for large scale optimization. *Math. Program.* **45**, 503–528 (1989)
14. A.F. Agarap, Deep learning using rectified linear units (relu). *CoRR*. [abs/1803.08375](https://arxiv.org/abs/1803.08375) (2018)
15. MLPRegressor Datasheet, [https://scikit-learn.org/stable/modules/generated/sklearn.neural\\_network.MLPRegressor.html](https://scikit-learn.org/stable/modules/generated/sklearn.neural_network.MLPRegressor.html)
16. M. Scholz et al., Concept of a compact high-resolution neutron spectrometer based on gem detector for fusion plasmas. *J. Instr.* **18**, C05001 (2023)

**Publisher's Note** Springer Nature remains neutral with regard to jurisdictional claims in published maps and institutional affiliations.